

Ionotropic GABA and glycine receptor subunit composition in human pluripotent stem cell-derived excitatory cortical neurones

Owain T. James^{1,2,3}, Matthew R. Livesey^{1,3}, Jing Qiu¹, Owen Dando^{1,2}, Bilada Bilican^{3,5,6}, Ghazal Haghi^{1,5}, Rinku Rajan^{1,5}, Karen Burr^{3,5,6}, Giles E. Hardingham^{1,4}, Siddharthan Chandran^{2,3,5,6}, Peter C. Kind^{1,2,4} and David J. A. Wyllie^{1,4}

¹Centre for Integrative Physiology, University of Edinburgh, Edinburgh EH8 9XD, UK

²Centre for Brain Development and Repair, Institute for Stem Cell Biology and Regenerative Medicine, National Centre for Biological Sciences, Bangalore 560065, India

³Euan MacDonald Centre for MND Research, University of Edinburgh, Edinburgh EH16 4SB, UK

⁴Patrick Wild Centre, University of Edinburgh, Edinburgh EH8 9XD, UK

⁵Centre for Clinical Brain Sciences, University of Edinburgh, Edinburgh EH16 4SB, UK

⁶MRC Centre for Regenerative Medicine, University of Edinburgh, Edinburgh EH16 4SB, UK

Key points

- This study reports a functional assessment of the subunit composition of inhibitory ionotropic GABA_A receptors (GABA_ARs) and glycine receptors (GlyRs) expressed by excitatory cortical neurones derived from human embryonic stem cells (hECNs).
- GABA_ARs expressed by hECNs are predominantly composed of $\alpha 2/3\beta 3\gamma 2$ subunits; such a composition is typical of that reported for GABA_ARs expressed in rodent embryonic cortex.
- Analysis of GlyRs expressed by hECNs indicates they are likely to contain $\alpha 2$ and β subunits – a composition in rodents that is associated with a late embryonic/early postnatal period of development.

Abstract We have assessed, using whole-cell patch-clamp recording and RNA-sequencing (RNA-seq), the properties and composition of GABA_A receptors (GABA_ARs) and strychnine-sensitive glycine receptors (GlyRs) expressed by excitatory cortical neurons derived from human embryonic stem cells (hECNs). The agonists GABA and muscimol gave EC₅₀ values of 278 μ M and 182 μ M, respectively, and the presence of a GABA_AR population displaying low agonist potencies is supported by strong RNA-seq signals for $\alpha 2$ and $\alpha 3$ subunits. GABA_AR-mediated currents, evoked by EC₅₀ concentrations of GABA, were blocked by bicuculline and picrotoxin with IC₅₀ values of 2.7 and 5.1 μ M, respectively. hECN GABA_ARs are predominantly γ subunit-containing as assessed by the sensitivity of GABA-evoked currents to diazepam and insensitivity to Zn²⁺, together with the weak direct agonist action of gaboxadol; RNA-seq indicated a predominant expression of the $\gamma 2$ subunit. Potentiation of GABA-evoked currents by propofol and etomidate and the lack of inhibition of currents by salicylidine salicylhydrazide (SCS) indicate expression of the $\beta 2$ or $\beta 3$ subunit, with RNA-seq analysis indicating strong expression of $\beta 3$ in hECN GABA_ARs. Taken together our data support the notion that hECN GABA_ARs have an $\alpha 2/3\beta 3\gamma 2$ subunit composition – a composition that also predominates in immature rodent cortex. GlyRs expressed by hECNs were activated by glycine with an EC₅₀ of 167 μ M. Glycine-evoked (500 μ M) currents were blocked by strychnine (IC₅₀ = 630 nM)

O. T. James and M. R. Livesey contributed equally to this work and are listed in alphabetical order.

and picrotoxin ($IC_{50} = 197 \mu M$), where the latter is suggestive of a population of heteromeric receptors. RNA-seq indicates GlyRs are likely to be composed of $\alpha 2$ and β subunits.

(Received 17 June 2014; accepted after revision 6 August 2014; first published online 28 August 2014)

Corresponding author D. J. A. Wyllie: Centre for Integrative Physiology, University of Edinburgh, Hugh Robson Building, George Square, Edinburgh EH8 9XD, UK. Email: dwyllie1@staffmail.ed.ac.uk

Abbreviations D-AP5, (2R)-amino-5-phosphonovaleric acid; CNQX, 6-cyano-7-nitroquinoxaline-2,3-dione; DIV, days *in vitro*; GABA_AR, γ -aminobutyric acid receptor type A; GFAP, glial fibrillary acidic protein; GlyR, glycine receptor; hECN, human excitatory cortical neurone; hPSC, human pluripotent stem cell; PCR, polymerase chain reaction; RNA-seq, RNA sequencing; VGLUT1, vesicular glutamate transporter 1.

Introduction

γ -Aminobutyric acid (GABA) type A receptors (GABA_ARs) are the principal inhibitory neurotransmitter receptors in the mammalian adult brain. GABA_ARs are a pentameric ligand-gated anion channels that can be potentially composed of 19 known subunits ($\alpha 1$ –6, $\beta 1$ –3, $\gamma 1$ –3, δ , ϵ , π , θ and $\rho 1$ –3), giving rise to a large number of potential receptor stoichiometries (Olsen & Sieghart, 2009). Alongside GABA_ARs, strychnine-sensitive glycine receptors (GlyRs) form another major class of pentameric ligand-gated anion channel that can be potentially composed of 5 subunits, $\alpha 1$ –4 and β (Lynch, 2009). GABA_AR and GlyR subunits are each associated with a high degree of spatial and developmental regulation within the CNS (Malosio *et al.* 1991; Laurie *et al.* 1992; Fritschy *et al.* 1994; Flint *et al.* 1998). In this regard, GABA_AR composition is currently limited to approximately 30 known variants. Moreover, subunit identity typically imparts various pharmacological specificities to the GABA_AR complex and, collectively, these properties make GABA_ARs a key pharmacological target for a range of neurological disorders (Olsen & Sieghart, 2009). The increasing knowledge regarding the functions of GlyRs within the developing CNS indicates that these receptors too are likely to be relevant pharmacological targets (Avila *et al.* 2013a).

The technological advance in the ability to generate human excitatory cortical neurones (hECNs) from pluripotent stem cells (hPSCs) gives the potential to study human-specific physiology and disease *in vitro*. We have previously reported a protocol that generates cultures of predominantly hECNs by 4 weeks of differentiation from anterior neural precursors derived from various stem cell lines (Bilican *et al.* 2014). The translational impact of this technology is ultimately determined by the ability of hECNs to display properties that reflect neurones in their native environment (Yang *et al.* 2011; Sandoe & Eggan, 2013). Indeed, we have previously identified that hECNs are a useful model to study the maturation of AMPAR composition and the reduction in intracellular Cl⁻ concentration that is observed in native neuronal development (Livesey *et al.* 2014). The present study

characterises the likely subunit composition of GABA_AR and GlyRs expressed by hECNs and illustrates that their subunit composition are likely to be similar to those that have been described for inhibitory ionotropic receptors expressed in immature rodent cortex.

Methods

In vitro hECN preparation

A detailed description of the derivation of hECNs can be found in Bilican *et al.* (2014). Briefly, hECNs were differentiated from anterior neural precursors that were derived from the H9 human embryonic stem cell line (WiCell), which was obtained under ethical/IRB approval of the University of Edinburgh. Experiments were carried out on cells that had been differentiated and maintained in culture for 28–42 days *in vitro* (DIV), or 49–56 DIV. At these time points, around 70% of cells were neuronal ($\beta 3$ -tubulin⁺), with little contamination from neural precursor cells (nestin⁺), astrocytes (GFAP⁺) or GABA-ergic (GAD65/67⁺) interneurons (Bilican *et al.* 2014; Livesey *et al.* 2014). Neurones were consistent with an excitatory (VGLUT1⁺) identity that also exhibited properties of neurones of the upper and lower layers of the cortex (see Bilican *et al.* 2014; Livesey *et al.* 2014).

Electrophysiology

The whole-cell patch-clamp configuration was used to record currents from hECNs using an Axon Multiclamp 700B amplifier (Molecular Devices, Sunnyvale, CA, USA). Patch electrodes (~4–7 M Ω) were filled with an 'internal' recording solution comprising (in mM): potassium gluconate 155, MgCl₂ 2, Na-HEPES 10, Na-PiCreatine 10, Mg₂-ATP 2 and Na₃-GTP 0.3, pH 7.3 (300 mOsmol l⁻¹). Coverslips containing hECNs were placed in the recording chamber, which was superfused with an 'external' recording solution composed of (in mM) NaCl 152, KCl 2.8, HEPES 10, CaCl₂ 2, glucose 10, pH 7.3 (320–330 mOsmol l⁻¹) using a gravity-feed system at room temperature (20–23°C) with a flow rate of approximately

4 ml min⁻¹. Time for complete bath solution exchange was approximately 5 s, but agonist onset times were dependent on position of perfusion line and cell; the rise-time of agonist-evoked whole-cell currents was < 2 s and all responses were measured at steady state. We observed that faster solution exchange rates were frequently associated with hECNs detaching from coverslips. The 'external' recording solution was supplemented with CNQX (5 μM), D-AP5 (50 μM), TTX (300 nM), and in the case of GABA_AR experiments, strychnine (20 μM). Recordings were made at a holding potential of 0 mV (-14 mV when corrected for the liquid junction potential), which gave a large driving force (~80 mV), resulting in inward flux of Cl⁻ ions. Series resistances (R_s) were between 10 and 30 MΩ and compensated between 50 and 80%. Experiments were terminated if series resistance shifted more than 20%.

Before each experiment, three bath applications of a given concentration of agonist that gave equivalent current amplitudes within 15% of the initial amplitude were obtained to establish a stable response. Similarly, a response to a control concentration of agonist was applied at the end of the recording to ensure stability. Data were only taken if the amplitude of the final control response was within 15% of the initial controls. Selective agonists, antagonists and allosteric modulators were purchased either from Tocris Bioscience (Bristol, UK) or Abcam (Cambridge, UK).

RNA-sequencing

For RNA-seq, RNA was isolated from four biological replicates using the Roche HP RNA Isolation kit according to manufacturer's instructions. Total RNA was assessed for quality (Agilent Bionalyzer) and quantity (Invitrogen Qubit) before library preparation. Illumina libraries were prepared from 1 μg of total RNA using TruSeq RNA Sample Prep Kit v2 with a 10 cycle enrichment step as per the manufacturer's recommendations. Final libraries were pooled in equimolar proportions before Illumina sequencing on a HiSeq 2500 platform using 100 base paired-end reads in rapid mode. Raw reads were processed using RTA 1.17.21.3 and Casava 1.8.2 (Illumina). Reads were mapped to the primary assembly of the human reference genome contained in Ensembl release 75. A genome index was built with Bowtie, version 1.0.0; default options; (Langmead *et al.* 2009), and then reads mapped with TopHat, version 2.0.10, (Kim *et al.* 2013); for TopHat, coverage-based search for junctions was disabled, otherwise default values were used for all options. Gene expression was then estimated with Cufflinks, version 2.2.0, (Trapnell *et al.* 2010; Roberts *et al.* 2011) using gene annotations from Ensembl release 75. Cufflinks was run in expression estimation mode only (-G flag), and corrections for multi-read mapping (-u flag) and bias

(-b flag) were enabled; otherwise default values were used for all options. Estimates of GABA_AR and GlyR subunit mRNA expression were then extracted in units of fragments per kilobase of exon per million mapped fragments, and normalised as expression relative to that of the highest expressed subunit.

Data analysis

Recordings were low-pass filtered at 2 kHz, digitised at 10 kHz *via* a BNC-2090A (National Instruments, TX, USA) interface, and recorded to computer using the WinEDR V2.7.6 Electrophysiology Data Recorder (J. Dempster, University of Strathclyde, UK, http://spider.science.strath.ac.uk/sipbs/software_ses.htm)

Agonist concentration-response curves were fitted individually for each cell using the Hill equation:

$$I = I_{\max}/(1 + (EC_{50}/[A])^{n_H}),$$

where I is the current response to agonist concentration $[A]$, n_H is the Hill coefficient, I_{\max} is the maximum current and EC_{50} is the concentration of agonist that produces a half-maximal response. Each data point was normalised to the fitted maximum of the concentration-response curve, then pooled, averaged and re-fitted again with the same equation, with the maximum and minimum for each curve being constrained to asymptote to 1 and 0, respectively (Frizelle *et al.* 2006; Wrighton *et al.* 2008).

Concentrations of antagonists required to inhibit agonist-evoked responses by 50% (IC_{50}) were determined by fitting inhibition curves with the equation:

$$I = I_{[B]0}/(1 + ([B]/IC_{50})^{n_H}),$$

where n_H is the Hill coefficient, $I_{[B]0}$ is the predicted current in the absence of antagonist and $[B]$ is the concentration of the antagonist. Data points were again normalised to the fitted maximum, before pooling, averaging and re-fitting as described above.

Data are presented as mean ± standard error of the mean (SEM). The number of experimental replicates (cells) is denoted as ' n ,' while ' N ' represents number of *de novo* preparations of batches from which ' n ' is obtained. Statistical analysis was conducted as described in the text with the significance levels indicated as: $P < 0.05$ (*), $P < 0.01$ (**) and $P < 0.001$ (***).

Results

GABA_A receptor characterisation

The potency of GABA_AR agonists varies considerably between GABA_AR isoforms (Mortensen *et al.* 2011; Karim *et al.* 2013). Thus, to characterise initially the functional properties of GABA_ARs expressed by

hECNs (28–42 DIV) differentiated from anterior neural precursors derived from H9 human embryonic stem cells (Bilican *et al.* 2014; see Methods) we conducted concentration–response experiments using GABA and the GABA_AR-selective agonist muscimol. We previously established that hECNs robustly respond to GABA at this time point (Livesey *et al.* 2014). After establishing stable control responses to bath applications of GABA (100 μ M), or muscimol (300 μ M), increasing concentrations of agonist were applied sequentially to generate concentration–response curves (Fig. 1A). Mean EC₅₀ values for GABA- and muscimol-activated currents were found to be $278 \pm 11 \mu$ M ($n = 12$, $N = 2$) and $182 \pm 10 \mu$ M ($n = 6$, $N = 2$), respectively (Fig. 1B). GABA (EC₅₀)-evoked current responses were blocked by

GABA_AR antagonists bicuculline and picrotoxin (Fig. 1C) in a concentration-dependent manner (Fig. 1D) giving respective IC₅₀ values of $2.7 \pm 0.2 \mu$ M ($n = 5$, $N = 2$) and $5.1 \pm 0.2 \mu$ M ($n = 4$, $N = 2$).

We next performed a series of pharmacological assays to assess the presence of γ and/or δ subunit-containing GABA_ARs. Applications of γ -selective allosteric potentiator diazepam (30 nM and 3 μ M) to GABA (EC₁₀; 35 μ M)-mediated currents potentiated the control GABA response by $10 \pm 6 \%$ ($P = 0.1$ vs. control) and $46 \pm 10 \%$ ($P < 0.001$ vs. control, Welch's *t* test, $n = 17$, $N = 3$), respectively, indicating the presence of the γ subunit (Fig. 2A). In contrast, applications of Zn²⁺ (10 μ M and 300 μ M), which selectively inhibits GABA_ARs composed of α and β subunits only (Draguhn *et al.* 1990), did not inhibit

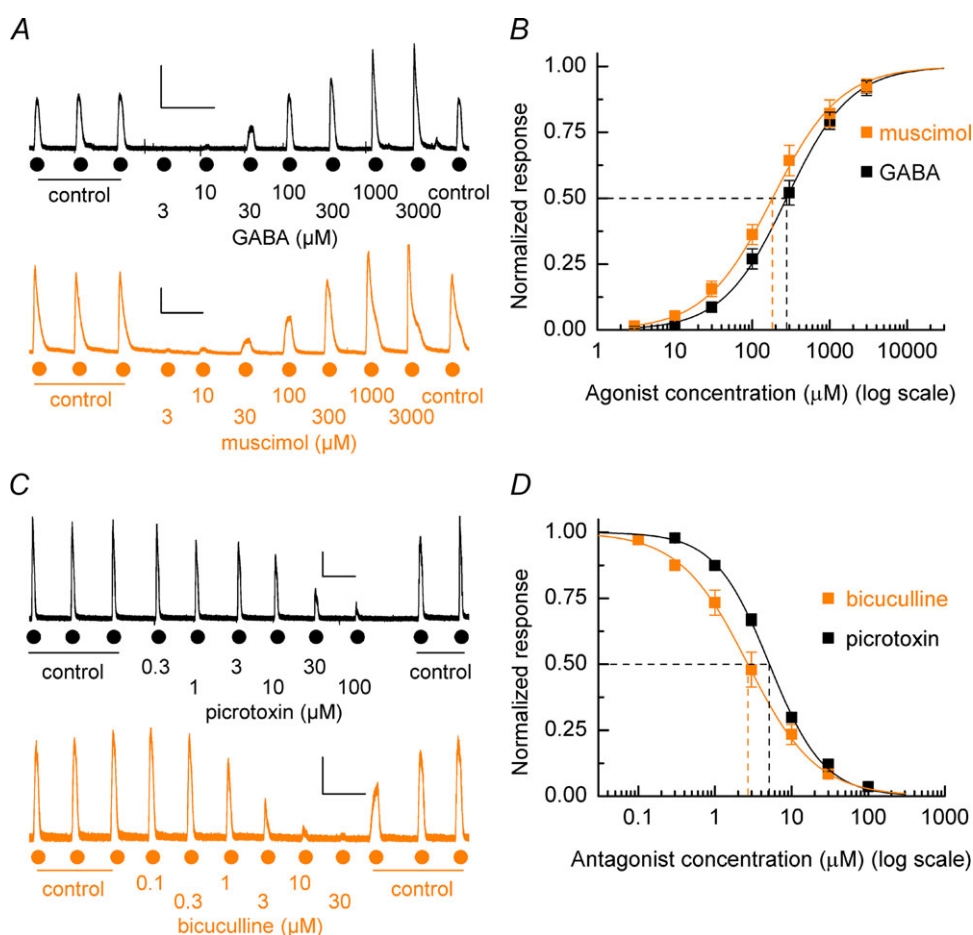


Figure 1. Agonist and antagonist pharmacology of hECN GABA_ARs

A, representative whole-cell current recordings of GABA and muscimol concentration–response experiments. Currents were elicited by increasing concentrations of bath applications of GABA and muscimol (3 μ M to 3 mM) after establishing 3 control GABA-evoked currents as indicated. Calibration bars 250 pA, 100 s. B, mean agonist concentration–response curves for GABA and muscimol. Mean GABA data: EC₅₀ = $278 \pm 11 \mu$ M, $n_H = 1.05 \pm 0.02$, $n = 12$, $N = 2$. Mean muscimol data: EC₅₀ = $182 \pm 10 \mu$ M; $n_H = 0.99 \pm 0.02$; $n = 6$, $N = 2$. C, example currents illustrating the inhibition of GABA-evoked responses by increasing concentrations of picrotoxin (upper panel) and bicuculline (lower panel). Calibration bars 250 pA, 100 s. D, mean inhibition curves for picrotoxin and bicuculline antagonism of GABA (EC₅₀) evoked currents. Mean bicuculline data: IC₅₀ = $2.7 \pm 0.2 \mu$ M; $n_H = 0.98 \pm 0.03$; $n = 5$, $N = 2$. Mean picrotoxin data: EC₅₀ = $5.1 \pm 0.2 \mu$ M; $n_H = 1.22 \pm 0.03$; $n = 4$, $N = 2$.

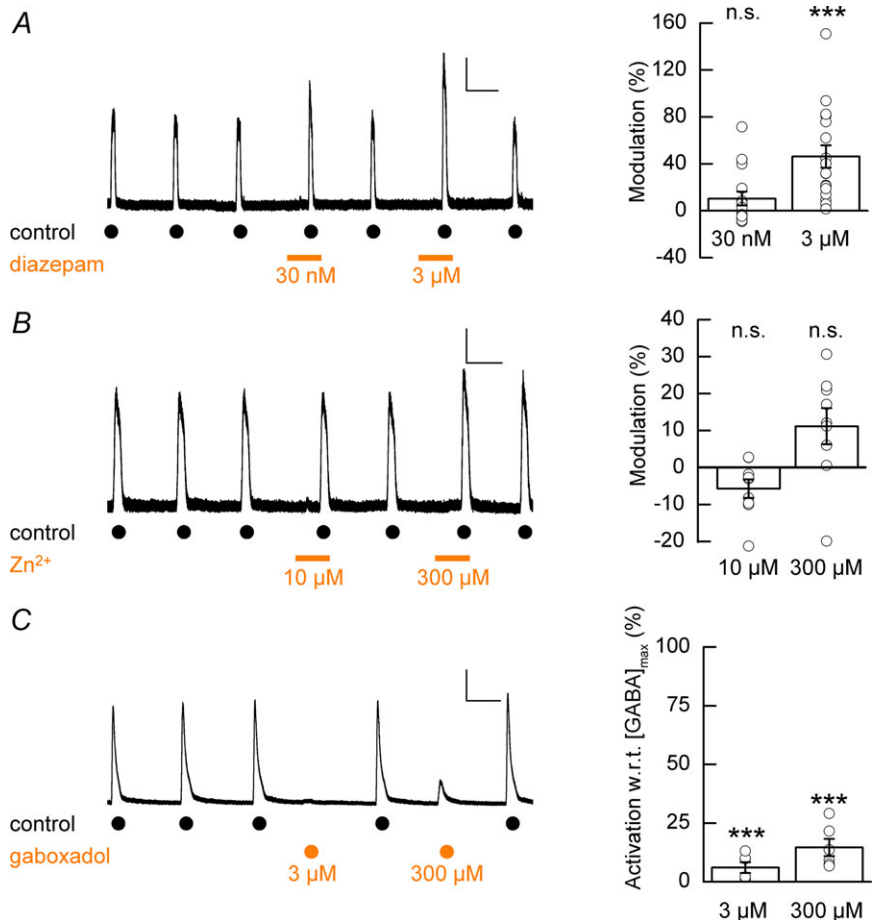
GABA (EC₅₀)-evoked currents (10 μ M, $6 \pm 3\%$, $P = 0.053$ vs. control; 300 μ M, $11 \pm 5\%$, $P = 0.052$ vs. control; unpaired t tests; $n = 9$, $N = 1$; Fig. 2B). Furthermore, the potent δ -containing GABA_AR-selective agonist gaboxadol (3 μ M and 300 μ M; Storustovu & Ebert, 2006) gave only nominal currents ($6.0 \pm 2.3\%$ and $14.6 \pm 3.7\%$; both data $P < 0.001$ vs. GABA (3 mM); unpaired t tests; $n = 6-7$, $N = 1$, respectively) compared to the maximum response that could be elicited by GABA (3 mM; Fig. 2C), confirming that a population of GABA_ARs that contain δ subunits is negligibly expressed. We confirmed that the low potency of GABA we observed was not a consequence of the specific culture conditions that we employed. Indeed GABA potency was not influenced by the culture of hECNs in atmospheric O₂ 48 h prior to recording (222 ± 13 μ M, $n = 3$, $N = 1$), the absence of brain-derived neurotrophic factor and glial cell-derived neurotrophic factor media supplements (222 ± 36 μ M, $n = 5$, $N = 2$), or maintaining hECNs for extended (49–56 DIV) culture periods (204 ± 17 μ M, $n = 5$, $N = 2$). Moreover, even for hECNs maintained for extended culture periods gaboxadol (300 μ M)-evoked currents remained very low ($9.7 \pm 4.1\%$, $n = 4$, $N = 1$) with respect to GABA-evoked currents and indicated that hECNs maintained in culture

for prolonged time periods (49–56 DIV) did not begin to express a δ -containing receptor population.

The presence of β subunits in hECN GABA_ARs was confirmed by the potentiation by the intravenous anaesthetic propofol (10 μ M) of GABA (EC₃₀; 120 μ M)-evoked currents which resulted in robust potentiation of the control current responses by $144\% \pm 29\%$ (Fig. 3A and B; $P = 0.002$ vs. control, unpaired t test, $n = 8$, $N = 2$; Sanna *et al.* 1995; Hill-Venning *et al.* 1997). Furthermore, direct activation of GABA_ARs was observed when propofol (100 μ M) was applied on its own ($98 \pm 21\%$ relative to GABA (EC₃₀; 120 μ M)-evoked control; $n = 7$, $N = 2$; Fig. 3A and C). The intravenous anaesthetic etomidate (3 μ M), which is selective for $\beta 2/3$ subunit-containing GABA_ARs (Hill-Venning *et al.* 1997), also potentiated GABA (EC₃₀; 120 μ M)-evoked currents by $75 \pm 20\%$ (Fig. 3A and B; $P = 0.01$ vs. control, unpaired t test, $n = 6$, $N = 1$) while application on its own and at a higher concentration (300 μ M) directly activated GABA_ARs ($116 \pm 23\%$ relative to GABA (EC₃₀; 120 μ M)-evoked control; $n = 6$, $N = 1$). Taken together, these data suggest the presence of a large complement of $\beta 2/3$ -containing GABA_ARs. The absence of $\beta 1$ -containing GABA_ARs was indicated by the fact that

Figure 2. Modulation of hECN GABA_ARs by diazepam, Zn²⁺ and gaboxadol

A, left panel: representative whole-cell recording depicting the co-application of diazepam (30 nM and 3 μ M, as indicated by bars) to control GABA-evoked responses. **A**, right panel: modulation of GABA_AR-mediated currents by diazepam (30 nM and 3 μ M, $n = 17$, $N = 3$). Data are presented as mean percentage modulation with respect to control recordings. No difference was observed between percentage modulation and the batch from which cells were prepared. Calibration bar 50 pA, 50 s. **B**, left panel: example whole-cell recording depicting the co-application of Zn²⁺ (10 μ M and 300 μ M, as indicated by bars) to control GABA-evoked responses. **B**, right panel: mean percentage modulation of control GABA_AR-mediated currents by Zn²⁺ ($n = 9$, $N = 1$). Calibration bar 100 pA, 50 s. **C**, left panel: example whole-cell recording of GABA (3 mM)-evoked currents and gaboxadol (3 μ M and 300 μ M)-induced currents. **C**, right panel: mean percentage gaboxadol-induced activation of GABA_AR currents with respect to (w.r.t.) maximum GABA-evoked currents ($n = 6-7$, $N = 1$). Calibration bar 500 pA, 50 s.



the selective inhibitor of $\beta 1$ -containing GABA_ARs, SCS (Thompson *et al.* 2004), failed to antagonise GABA (EC₃₀; 120 μ M)-evoked currents (Fig. 3A and B; SCS *vs.* control, $P = 0.27$ *vs.* control, unpaired *t* test, $n = 8$, $N = 2$).

As illustrated above GABA-evoked currents are potentiated by diazepam which suggests that $\alpha 4$ and $\alpha 6$ subunits are absent from the GABA_AR population in hECNs since typically benzodiazepines are active at $\alpha 1$,

$\alpha 2$, $\alpha 3$, or $\alpha 5$ -containing GABA_ARs (Olsen & Sieghart, 2009). To rule out the possibility of the expression of $\alpha 4$ and $\alpha 6$ subunits, GABA (EC₃₀; 120 μ M)-elicited currents were shown to be insensitive to the $\alpha 4/\alpha 6$ subunit containing GABA_AR inhibitor furosemide (100 μ M; $P = 0.43$ *vs.* control, unpaired *t* test, $n = 6$, $N = 2$; Fig. 3D and E; Knoflach *et al.* 1996; Wafford *et al.* 1996). Furthermore, the observed low GABA and muscimol

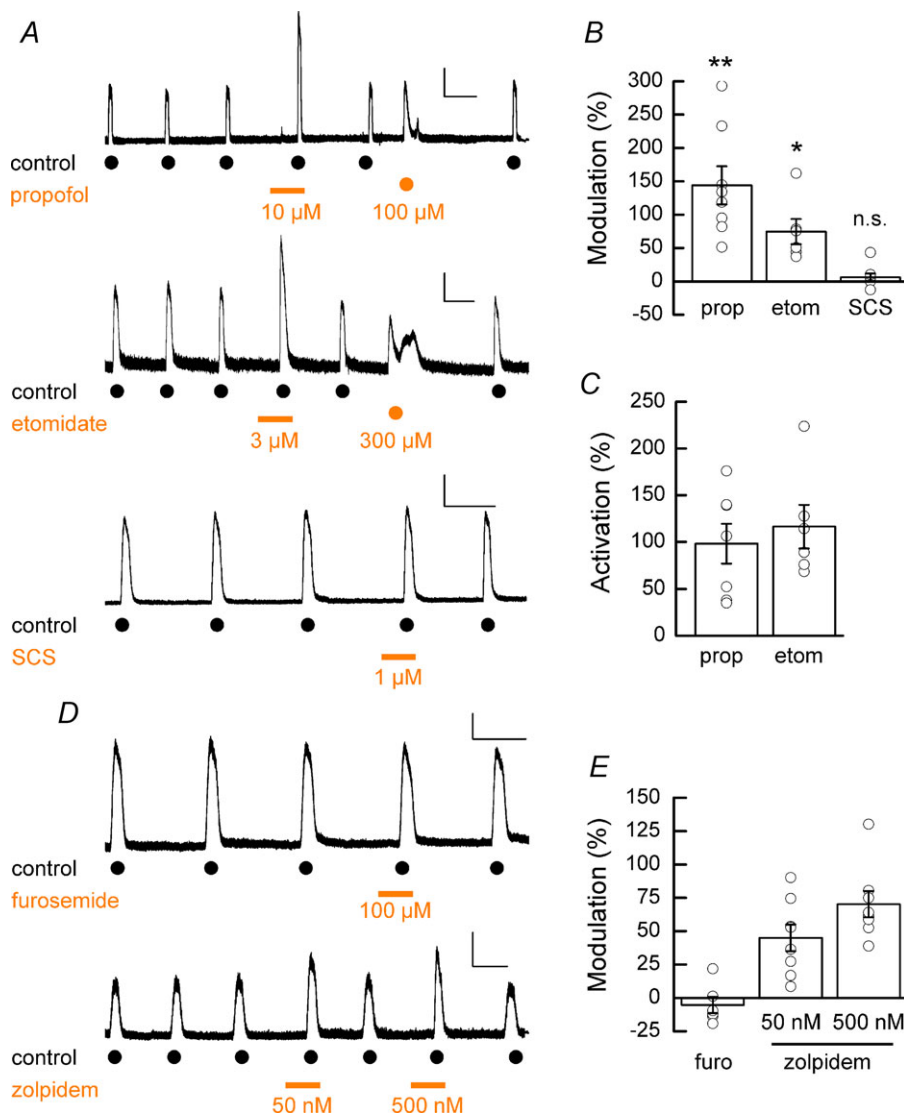


Figure 3. Modulation of hECN GABA_ARs by intravenous anesthetics, SCS, furosemide and zolpidem
 A, upper panel: example trace showing potentiation of GABA-mediated whole-cell currents and direct activation of GABA_ARs by propofol. A, middle panel: example trace showing potentiation of GABA-mediated whole-cell currents and direct activation of GABA_ARs by etomidate. A, lower panel: example trace showing lack of inhibition of GABA-mediated whole-cell currents by SCS. Calibration bars: 100 pA, 50 s (upper); 100 pA, 50 s (middle); 250 pA, 50 s (lower). B, mean percentage modulation GABA-induced currents by the allosteric modulators propofol (10 μ M; $n = 8$, $N = 2$), etomidate (3 μ M; $n = 6$, $N = 1$) and SCS (1 μ M; $n = 8$, $N = 2$). C, mean percentage direct activation propofol and etomidate expressed with respect to control responses to GABA. D, upper panel: example trace showing lack of inhibition of GABA-mediated whole-cell currents by furosemide. D, lower panel: example trace showing potentiation of GABA-mediated whole-cell currents by zolpidem ($n = 6$ – 8 , $N = 2$ for each condition). Calibration bars: 150 pA, 50 s (upper); 100 pA, 50 s (lower). E, mean percentage modulation GABA-induced currents by the allosteric modulators furosemide (100 μ M) and zolpidem (50 nM and 500 nM).

potencies (Fig. 1B) argues against the expression of $\alpha 4$ and $\alpha 6$ subunits, and also $\alpha 5$ subunits, which typically display high GABA potency (Mortensen *et al.* 2011; Karim *et al.* 2013). To identify the nature of the α subunit we examined the actions of zolpidem (50 nM and 500 nM), which exhibits selectivity for $\alpha 1$ -containing GABA_ARs with lesser potency at $\alpha 2$ - and $\alpha 3$ -containing GABA_ARs and negligible activity at $\alpha 5$ -containing GABA_ARs (Sanna *et al.* 2002). Co-application of zolpidem to GABA (EC₁₀; 35 μ M)-evoked currents resulted in only a mild potentiation of control currents (Fig. 3D and E; 50 nM: 46 \pm 10%; 500 nM: 70 \pm 10%, $n = 8$, $N = 2$), indicating the majority of the GABA_AR population expressed by hECNs most likely contain $\alpha 2$ and/or $\alpha 3$ subunits.

To assess quantitatively the expression of GABA_AR subunits we examined the relative expression of subunit mRNA transcripts via RNA-seq analysis (35 DIV). Figure 4A shows the relative expression of α , β and γ subunits with levels normalised to the highest expressed subunit mRNA ($\beta 3$). These data are consistent with the pharmacological analysis of GABA_ARs expressed by hECNs described above. For α subunits, we found prominent mRNA expression of the $\alpha 2$ and $\alpha 3$ subunits and very little detection of $\alpha 4$ and $\alpha 6$ subunits, whilst the $\alpha 1$ and $\alpha 5$ subunit mRNAs were expressed to a moderate extent. The $\beta 3$ subunit is prominently expressed over $\beta 1$ and $\beta 2$ subunits. Pharmacological data do not point to the identity of the γ subunit(s) that are functionally expressed by hECNs; however, the RNA-seq data indicate the strongest expression of the $\gamma 2$ subunit mRNA. In agreement with the pharmacological analysis, levels of δ subunit mRNA expression were considered to be nominal.

Strychnine-sensitive glycine receptor characterisation

GlyR characterisation was initially performed with RNA-seq analysis of GlyR subunit mRNA transcripts in hECNs (35 DIV; Fig. 4B). Both $\alpha 2$ and β subunits are abundantly expressed at the mRNA level, whilst $\alpha 1$ and $\alpha 3$ subunits are only nominally or weakly expressed, respectively, relative to the $\alpha 2$ subunit. As expected, the presence of $\alpha 4$ subunit mRNA was not detected given its status as a pseudogene in humans (Lynch, 2009).

Functional expression of GlyRs was examined by the ability of hECNs (7–35 DIV) to respond to bath applications of glycine (500 μ M). With increasing periods following differentiation the mean GlyR-mediated current density profile displays a marked increase (Fig. 5A; 3.3 \pm 2.2 pA pF⁻¹ to 49.4 \pm 8.4 pA pF⁻¹; $P < 0.001$, unpaired t test, $n = 7$, $N = 2$), indicating a strong temporal up-regulation of functional GlyRs expressed by hECNs. Furthermore by 28 DIV all cells examined gave currents (Fig. 5A) and in all cases examined these were blocked by the GlyR antagonist strychnine (20 μ M).

The potency of glycine-evoked currents was assessed by concentration–response experiments (Fig. 5B), from which a curve-fitting of mean data yielded an EC₅₀ of 167 \pm 20 μ M (Fig. 5C). Glycine-evoked (500 μ M) currents were blocked fully by strychnine in a concentration-dependent manner with an IC₅₀ of 630 \pm 59 nM ($n = 5$, $N = 2$; Fig. 5D and E). Note that an increased agonist concentration, rather than the typical EC₅₀, was used to elicit suitable current responses to measure antagonist effects. The composition of the expressed GlyRs was probed using picrotoxin, which exhibits selectivity for homomeric over heteromeric GlyR forms, as the inclusion of the β subunit into the GlyR results in a reduction in sensitivity to picrotoxin (Pribilla *et al.* 1992; Wang *et al.* 2006; Lynch, 2009). Inhibition of GlyRs by picrotoxin (Fig. 5D and E) gave an IC₅₀ of 197 \pm 22 μ M ($n = 5$, $N = 2$), indicating the low potency of this antagonist at hECN GlyRs and suggesting that the majority of these receptors are heteromeric assemblies contain α and β subunits.

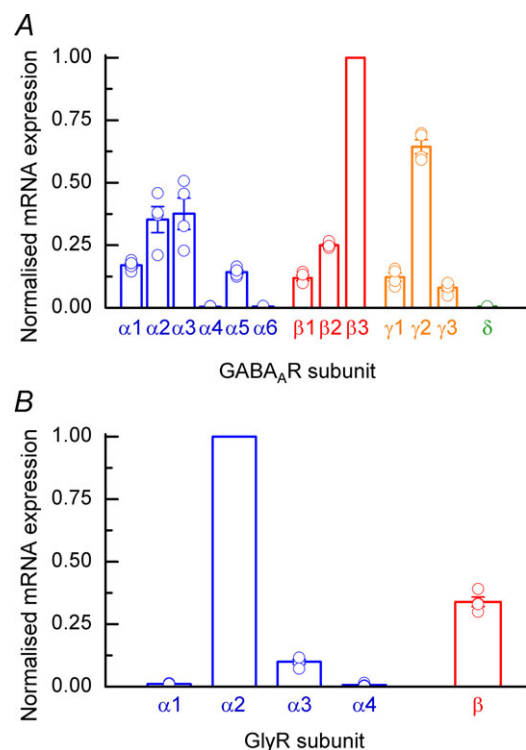


Figure 4. RNA-seq analysis of GABA_AR and GlyR subunits

A, mean human GABA_AR subunit mRNA estimated abundances ($N = 4$) derived from RNA-seq analysis of hECNs (DIV 35). Data are normalised to the largest mRNA signal ($\beta 3$ subunit). The relative expression of other GABA_AR subunits (ϵ , π , θ and σ) gave signals that were considered to reflect the absence of mRNA for these subunits. B, RNA-seq analysis human GlyR subunits as described in A. Data are normalised as expression relative to $\alpha 2$ subunit mRNA signal.

Discussion

We have employed a variety of techniques to identify the principal subunit composition of ionotropic GABA_ARs and GlyRs expressed by hECNs. The identification of GABA_AR subunit regulation and expression is relevant to neurodevelopment and neurological disease and thus the ability of hPSC-derived neurones to express GABA_ARs that reflect those seen in native neurones is essential if such *in vitro* preparations are to be used for human-specific development and disease modelling.

Our data establish that the predominant GABA_AR α subunits expressed by hECNs (DIV 28–45) are $\alpha 2$ and/or $\alpha 3$ subunits, which is consistent with an expression profile predominantly exhibited by embryonic rodent

cortical neurones (Laurie *et al.* 1992; Fritschy *et al.* 1994). Given that GABA-evoked currents were not inhibited by furosemide, hECN GABA_ARs are considered to lack $\alpha 4$ and $\alpha 6$ subunits. Furthermore, the mild modulatory action of zolpidem suggests the absence of the $\alpha 1$ subunit which is perhaps to be expected given that this subunit is associated with a more mature neuronal phenotype (Laurie *et al.* 1992; Fritschy *et al.* 1994). In agreement with our pharmacological analysis, RNA-seq also showed only moderate expression of $\alpha 1$ subunits together with negligible expression of both $\alpha 4$ and $\alpha 6$ subunits compared to the relative abundance of transcripts for both $\alpha 2$ and $\alpha 3$ subunits. We considered that the functional expression of the $\alpha 5$ subunit, which is associated with high agonist potency, was unlikely given

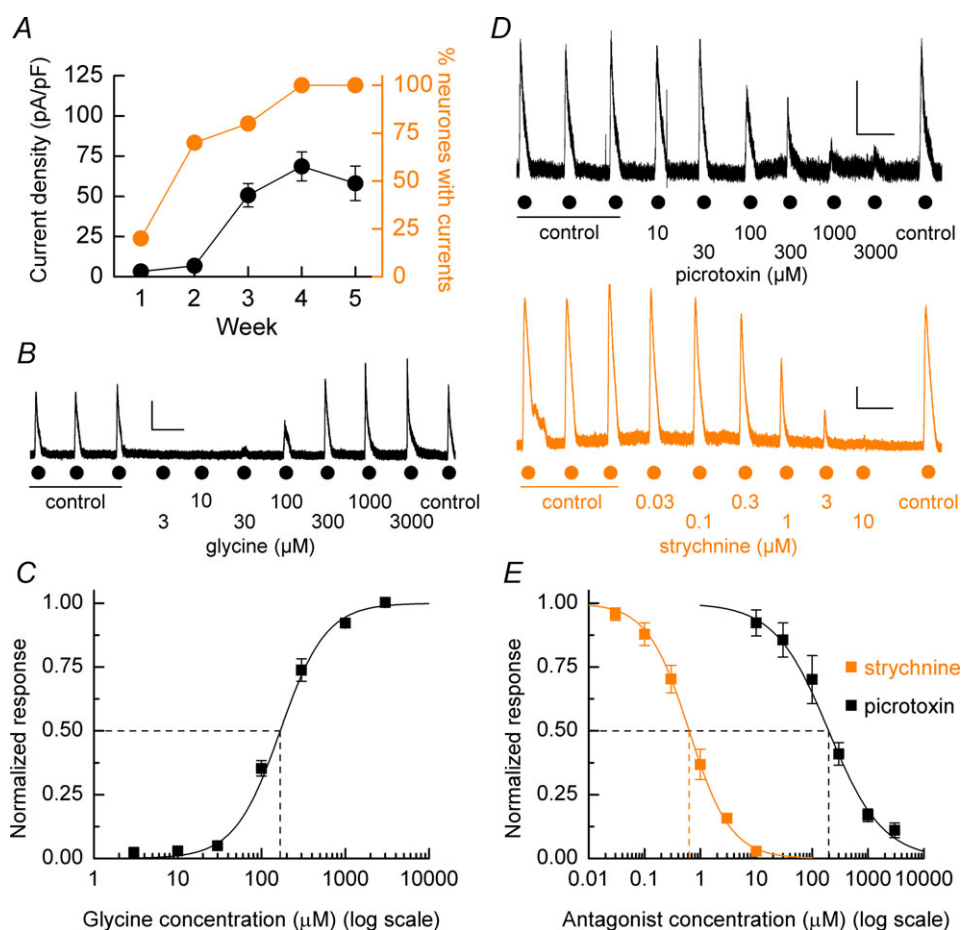


Figure 5. Agonist and antagonist pharmacology of hECN GlyRs

A, weekly percentage response to bath applications of glycine and the mean glycine-mediated current density. $n = 25\text{--}31$, $N = 3$. *B*, representative whole-cell current recordings of glycine concentration–response experiments. Currents were elicited by increasing concentrations of glycine after establishment of 3 control glycine-evoked currents. Calibration bar 125 pA, 50 s. *C*, mean (\pm SEM) agonist concentration–response curve for glycine. Mean glycine data: $\text{EC}_{50} = 167 \pm 20 \mu\text{M}$; $n_{\text{H}} = 1.59 \pm 0.1$; $n = 7$, $N = 2$. *D*, upper panel: example current recording of the inhibition of glycine-evoked (500 μM) responses by increasing concentrations of picrotoxin. *D*, lower panel: strychnine inhibition of glycine-evoked (500 μM) currents amplitudes. Calibration bars 125 pA, 50 s. *E*, mean inhibition curves for picrotoxin and strychnine antagonism of glycine-evoked currents. Mean picrotoxin data: $\text{IC}_{50} = 197 \pm 22 \mu\text{M}$; $n_{\text{H}} = 0.9 \pm 0.06$; $n = 5$, $N = 2$. Mean strychnine data: $\text{EC}_{50} = 690 \pm 59 \text{ nM}$; $n_{\text{H}} = 1.17 \pm 0.06$; $n = 5$, $N = 2$.

the relatively low levels of mRNA detected and the low agonist potencies of GABA and muscimol. Indeed, low potency is indicative of GABA_ARs that contain either $\alpha 2$ or $\alpha 3$ subunits (Mortensen *et al.* 2011; Karim *et al.* 2013).

High expression of the GABA_AR $\beta 3$ subunit has been associated with rodent immature cortical neurones (Laurie *et al.* 1992), though the $\beta 2$ subunit is often also reported to be substantially expressed in cortical neurones (Fritschy *et al.* 1994). Potentiation of GABA-evoked currents by the low concentrations of intravenous anaesthetics etomidate and propofol, direct activation by high concentrations of etomidate and propofol, a lack of SCS inhibition and a high level of mRNA expression for the $\beta 3$ subunit collectively demonstrate that hECNs are likely to predominantly express $\beta 3$ subunit-containing GABA_ARs, although a contribution of $\beta 2$ to GABA_AR stoichiometry cannot be ruled out.

The vast majority of GABA_ARs in the CNS are $\gamma 2$ subunit containing (Olsen & Sieghart, 2009). RNA-seq data indicate that hECNs predominantly express the $\gamma 2$ subunit, in agreement with the pharmacological findings that GABA-evoked currents were potentiated by γ subunit-selective diazepam. Subsets of δ subunit-containing GABA_ARs are selectively expressed by certain cortical adult neuronal phenotypes and importantly are commonly associated with GABA_AR-mediated tonic inhibition (Olsen & Sieghart, 2009). Nevertheless, our data indicate that hECNs lack δ subunit-containing GABA_ARs as gaboxadol gave rise to only low amplitude currents compared to those seen with GABA. Furthermore, the finding that Zn²⁺ did not inhibit GABA-evoked currents is consistent with the absence of GABA_ARs containing *only* α/β subunits.

We have demonstrated that both RNA-seq analysis and selective GABA_AR pharmacology converge on a predominant GABA_AR composition of $\alpha 2/3\beta 3\gamma 2$. Such isoforms are observed in recombinant expression systems to have low agonist potency relative to other isoforms and we similarly demonstrate that GABA_AR expressed upon hECNs exhibit relatively low agonist potency (Karim *et al.* 2013). This GABA_AR isoform is the most likely to be widely expressed in the immature rodent cortex (Laurie *et al.* 1992; Olsen & Sieghart, 2009). Nevertheless, our data cannot rule out the presence of other GABA_AR isoforms expressed at a low level. However, inspection of Brainspan (Atlas of the Developing Human Brain <http://www.brainspan.org/rnaseq/search>) indicates that the levels of mRNA we report from the RNA-seq analysis of hECNs (35 DIV) are qualitatively similar to those seen in human cortical neurones between 12 and 21 weeks post conception. Thus, hECNs provide a system to investigate the properties of human GABA_AR pharmacology and furthermore permit investigation of the role of GABA_ARs in the maturing cortical neurones (Wang & Kriegstein, 2009).

In rodents, transient functional GlyR expression is a key feature of early neocortical development (Flint *et al.* 1998; Avila *et al.* 2013a). Indeed, hECNS maintained for 28–42 DIV exhibited strong responses to glycine that were blocked by the GlyR antagonist strychnine. Glycine concentration–response experiments indicated glycine potency was lower than previously reported recombinant values (Pribilla *et al.* 1992) but is generally higher than glycine potencies observed in native cortical preparations (Flint *et al.* 1998; Okabe *et al.* 2004; Kilb *et al.* 2008; but see Avila *et al.* 2013b). The reasons for these differences are unknown, but may be related to systematic differences in the solution exchange times of these studies, where slower exchange times are more likely to give shallower observed concentration–response curves. In this regard, the ability to examine deactivation kinetics of GlyRs expressed by hECNs in isolated patches using fast agonist application may yield further details of GlyR identity (Mangin *et al.* 2003; Pitt *et al.* 2008; Krashia *et al.* 2011; Marabelli *et al.* 2013).

GlyRs expressed by rodent forebrain neurones have been described as developing from an embryonic homomeric to postnatal heteromeric (β subunit-containing) composition (Lynch, 2009). To investigate the functional GlyR composition we used the antagonist picrotoxin, which inhibits homomeric over heteromeric GlyRs (Lynch, 2009). Given the observed low sensitivity of GlyRs to picrotoxin, our results suggest that the principal GlyR identity of hECNs is likely to a heteromeric α/β assembly. Pharmacological tools to identify unambiguously the nature of the α subunit within the heteromer are lacking (but see Han *et al.* 2004); however, RNA-seq analysis indicates that $\alpha 2$ subunit mRNA is the most abundantly expressed. As is the case for GABA_AR subunit expression, levels of mRNA expression for GlyRs in our RNA-seq analysis are consistent with a development age of around 12–21 weeks post conception (Atlas of the Developing Human Brain <http://www.brainspan.org/rnaseq/search>). Finally, it is of interest to note that there is transient expression of heteromeric $\alpha 2/\beta$ GlyRs by rodent Cajal–Retzius cells in early postnatal development (Okabe *et al.* 2004). This class of neurone is considered to form a significant population in our hECN cultures (Bilican *et al.* 2014) and in this respect hECNs may provide a useful human model of GlyR development.

References

- Avila A, Nguyen L & Rigo JM (2013a). Glycine receptors and brain development. *Front Cell Neurosci* 7, 184.
- Avila A, Vidal PM, Dear TN, Harvey RJ, Rigo JM & Nguyen L (2013b). Glycine receptor $\alpha 2$ subunit activation promotes cortical interneuron migration. *Cell Rep* 4, 738–750.

- Bilican B, Livesey MR, Haghi G, Qiu J, Burr K, Siller R, Hardingham GE, Wyllie DJ & Chandran S (2014). Physiological normoxia and absence of EGF is required for the long-term propagation of anterior neural precursors from human pluripotent cells. *Plos One* **9**, e85932.
- Draguhn A, Verdorn TA, Ewert M, Seeburg PH & Sakmann B (1990). Functional and molecular distinction between recombinant rat GABA_A receptor subtypes by Zn²⁺. *Neuron* **5**, 781–788.
- Flint AC, Liu X & Kriegstein AR (1998). Nonsynaptic glycine receptor activation during early neocortical development. *Neuron* **20**, 43–53.
- Fritschy JM, Paysan J, Enna A & Mohler H (1994). Switch in the expression of rat GABA_A-receptor subtypes during postnatal development: an immunohistochemical study. *J Neurosci* **14**, 5302–5324.
- Frizelle PA, Chen PE & Wyllie DJ (2006). Equilibrium constants for (R)-[(S)-1-(4-bromo-phenyl)-ethylamino]-(2,3-dioxo-1,2,3,4-tetrahydroquinoxalin-5-yl)-methyl]-phosphonic acid (NVP-AAM077) acting at recombinant NR1/NR2A and NR1/NR2B N-methyl-D-aspartate receptors: Implications for studies of synaptic transmission. *Mol Pharmacol* **70**, 1022–1032.
- Han Y, Li P & Slaughter MM (2004). Selective antagonism of rat inhibitory glycine receptor subunits. *J Physiol* **554**, 649–658.
- Hill-Venning C, Belelli D, Peters JA & Lambert JJ (1997). Subunit-dependent interaction of the general anaesthetic etomidate with the gamma-aminobutyric acid type A receptor. *Br J Pharmacol* **120**, 749–756.
- Karim N, Wellendorph P, Absalom N, Johnston GA, Hanrahan JR & Chebib M (2013). Potency of GABA at human recombinant GABA_A receptors expressed in *Xenopus* oocytes: a mini review. *Amino Acids* **44**, 1139–1149.
- Kilb W, Hanganu IL, Okabe A, Sava BA, Shimizu-Okabe C, Fukuda A & Luhmann HJ (2008). Glycine receptors mediate excitation of subplate neurons in neonatal rat cerebral cortex. *J Neurophysiol* **100**, 698–707.
- Kim D, Perteua G, Trapnell C, Pimentel H, Kelley R & Salzberg SL (2013). TopHat2: accurate alignment of transcriptomes in the presence of insertions, deletions and gene fusions. *Genome Biol* **14**, R36.
- Knoflach F, Benke D, Wang Y, Scheurer L, Luddens H, Hamilton BJ, Carter DB, Mohler H & Benson JA (1996). Pharmacological modulation of the diazepam-insensitive recombinant γ -aminobutyric acid_A receptors $\alpha 4\beta 2\gamma 2$ and $\alpha 6\beta 2\gamma 2$. *Mol Pharmacol* **50**, 1253–1261.
- Krashia P, Lape R, Lodesani F, Colquhoun D & Sivilotti LG (2011). The long activations of $\alpha 2$ glycine channels can be described by a mechanism with reaction intermediates (“flip”). *J Gen Physiol* **137**, 197–216.
- Langmead B, Trapnell C, Pop M & Salzberg SL (2009). Ultrafast and memory-efficient alignment of short DNA sequences to the human genome. *Genome Biol* **10**, R25.
- Laurie DJ, Wisden W & Seeburg PH (1992). The distribution of thirteen GABA_A receptor subunit mRNAs in the rat brain. III. Embryonic and postnatal development. *J Neurosci* **12**, 4151–4172.
- Livesey MR, Bilican B, Qiu J, Rzechorzek NM, Haghi G, Burr K, Hardingham GE, Chandran S & Wyllie DJ (2014). Maturation of AMPAR composition and the GABA_AR reversal potential in hPSC-derived cortical neurons. *J Neurosci* **34**, 4070–4075.
- Lynch JW (2009). Native glycine receptor subtypes and their physiological roles. *Neuropharmacology* **56**, 303–309.
- Malosio ML, Marqueze-Pouey B, Kuhse J & Betz H (1991). Widespread expression of glycine receptor subunit mRNAs in the adult and developing rat brain. *EMBO J* **10**, 2401–2409.
- Mangin JM, Baloul M, Prado De Carvalho L, Rogister B, Rigo JM & Legendre P (2003). Kinetic properties of the $\alpha 2$ homo-oligomeric glycine receptor impairs a proper synaptic functioning. *J Physiol* **553**, 369–386.
- Marabelli A, Moroni M, Lape R & Sivilotti LG (2013). The kinetic properties of the $\alpha 3$ rat glycine receptor make it suitable for mediating fast synaptic inhibition. *J Physiol* **591**, 3289–3308.
- Mortensen M, Patel B & Smart TG (2011). GABA Potency at GABA_A receptors found in synaptic and extrasynaptic zones. *Front Cell Neurosci* **6**, 1.
- Okabe A, Kilb W, Shimizu-Okabe C, Hanganu IL, Fukuda A & Luhmann HJ (2004). Homogenous glycine receptor expression in cortical plate neurons and Cajal–Retzius cells of neonatal rat cerebral cortex. *Neuroscience* **123**, 715–724.
- Olsen RW & Sieghart W (2009). GABA_A receptors: subtypes provide diversity of function and pharmacology. *Neuropharmacology* **56**, 141–148.
- Pitt SJ, Sivilotti LG & Beato M (2008). High intracellular chloride slows the decay of glycinergic currents. *J Neurosci* **28**, 11454–11467.
- Pribilla I, Takagi T, Langosch D, Bormann J & Betz H (1992). The atypical M2 segment of the beta subunit confers picrotoxinin resistance to inhibitory glycine receptor channels. *EMBO J* **11**, 4305–4311.
- Roberts A, Trapnell C, Donaghey J, Rinn JL & Pachter L (2011). Improving RNA-Seq expression estimates by correcting for fragment bias. *Genome Biol* **12**, R22.
- Sandoe J & Eggan K (2013). Opportunities and challenges of pluripotent stem cell neurodegenerative disease models. *Nat Neurosci* **16**, 780–789.
- Sanna E, Busonero F, Talani G, Carta M, Massa F, Peis M, Maciocco E & Biggio G (2002). Comparison of the effects of zaleplon, zolpidem, and triazolam at various GABA_A receptor subtypes. *Eur J Pharmacol* **451**, 103–110.
- Sanna E, Mascia MP, Klein RL, Whiting PJ, Biggio G & Harris RA (1995). Actions of the general anesthetic propofol on recombinant human GABA_A receptors: influence of receptor subunits. *J Pharmacol Exp Ther* **274**, 353–360.
- Storustovu SI & Ebert B (2006). Pharmacological characterization of agonists at δ -containing GABA_A receptors: Functional selectivity for extrasynaptic receptors is dependent on the absence of $\gamma 2$. *J Pharmacol Exp Ther* **316**, 1351–1359.
- Thompson SA, Wheat L, Brown NA, Wingrove PB, Pillai GV, Whiting PJ, Adkins C, Woodward CH, Smith AJ, Simpson PB, Collins I & Wafford KA (2004). Salicylidene salicylhydrazide, a selective inhibitor of $\beta 1$ -containing GABA_A receptors. *Br J Pharmacol* **142**, 97–106.

- Trapnell C, Williams BA, Pertea G, Mortazavi A, Kwan G, van Baren MJ, Salzberg SL, Wold BJ & Pachter L (2010). Transcript assembly and quantification by RNA-Seq reveals unannotated transcripts and isoform switching during cell differentiation. *Nat Biotechnol* **28**, 511–515.
- Wafford KA, Thompson SA, Thomas D, Sikela J, Wilcox AS & Whiting PJ (1996). Functional characterization of human γ -aminobutyric acid_A receptors containing the α 4 subunit. *Mol Pharmacol* **50**, 670–678.
- Wang DD & Kriegstein AR (2009). Defining the role of GABA in cortical development. *J Physiol* **587**, 1873–1879.
- Wang DS, Mangin JM, Moonen G, Rigo JM & Legendre P (2006). Mechanisms for picrotoxin block of α 2 homomeric glycine receptors. *J Biol Chem* **281**, 3841–3855.
- Wrighton DC, Baker EJ, Chen PE & Wyllie DJ (2008). Mg²⁺ and memantine block of rat recombinant NMDA receptors containing chimeric NR2A/2D subunits expressed in *Xenopus laevis* oocytes. *J Physiol* **586**, 211–225.
- Yang N, Ng YH, Pang ZP, Sudhof TC & Wernig M (2011). Induced neuronal cells: how to make and define a neuron. *Cell Stem Cell* **9**, 517–525.

Additional Information

Competing interests

The authors declare no conflict of interest.

Author contributions

Conception and design of the experiments: O.T.J., M.R.L., J.Q., O.D., G.E.H., S.C., P.C.K. and D.J.A.W. Collection, analysis and interpretation of data: O.T.J., M.R.L., J.Q., O.D., B.B., G.H., R.R.,

K.B. and D.J.A.W. Drafting the article or revising it critically for important intellectual content: O.T.J., M.R.L., O.D., G.E.H., S.C., P.C.K. and D.J.A.W. It is confirmed that all authors approved the final version of the manuscript and that all persons designated as authors qualify for authorship, and all those who qualify for authorship are listed. All experiments were performed in the laboratories of G.E.H., S.C., P.C.K. and D.J.A.W at the University of Edinburgh, Edinburgh, UK.

Funding

This research was funded by The Wellcome Trust (Grant 092742/Z/10/Z to D.J.A.W., S.C. and G.E.H.), the Medical Research Council (Senior Non-clinical Research Fellowship to G.E.H.), the Euan MacDonald Centre and the NC3Rs CRACK IT Programme (S.C.) and seedcorn funding from the Patrick Wild Centre/RS Macdonald Trust (P.C.K. and D.J.A.W).

Acknowledgements

We thank Karim Gharbi and Timothee Cezard (Edinburgh Genomics, University of Edinburgh) for their help in conducting RNA-seq analysis and the members of our lab for their many constructive comments during the course of this study.

Authors' present addresses

G. Haghi: New World Laboratories, 500 Cartier Blvd, Laval, H7V 5B7, Quebec, Canada. B. Bilican: Novartis Institutes for Biomedical Research, 100 Technology Square, Cambridge, MA 02139, USA.